A SunCam online continuing education course

Precision Measurement

by

Tony L. Schmitz, PhD

2. Precision Measurement

(Displacement Measuring Interferometry)

Since its introduction in the mid-1960s, displacement measuring interferometry has offered high accuracy, range, and resolution for non-contact displacement measurement applications. Important examples include: 1) positional feedback of precision stages on photolithographic steppers for integrated circuit fabrication; 2) transducer calibration; 3) positional feedback for machine tools, coordinate measuring machines, and other metrology systems; and error measurement for these same machines. A common configuration choice in these situations is the heterodyne (or two frequency) Michelson-type interferometer with single, double, or multiple passes of the optical paths. These systems infer changes in displacement of a selected optical path by monitoring the optically induced variation in the photodetector current, which is generated from the optical interference signal. The phase measuring electronics convert this photodetector current to displacement using an assumed relationship between corresponding changes in detector current and displacement, where this relationship is defined by idealized performance of the optical elements. In this course, the fundamentals of displacement measuring interferometer are outlined for those engineers who may be interested in implementing this technology.

2.1 Introduction

A logical starting point in a discussion of displacement measuring interferometry is a brief review of the fundamentals of light theory, polarization, and interference. Light is a transverse electromagnetic wave with well-established relationships between the velocity, wavelength and frequency. The velocity of light in a given medium, v, is related to the speed of light in vacuum, c, by the index of refraction, n. This relationship is given in Eq. 2.1.1. A similar relationship can be seen between the wavelength of light in a given medium, λ, and the wavelength in a vacuum, λ_o. See Eq. 2.1.2. At standard temperature and pressure (temperature = 20°C, pressure = 760 mm Hg, relative humidity = 50%), the index of refraction of air is 1.000271296 [1]. The velocity of light in air is, therefore, slightly less than the velocity of light in vacuum.

$$v = c / n, \qquad \text{where } c = 2.99792458e8 \text{ m/s} \tag{2.1.1}$$

$$\lambda = \lambda_o / n \tag{2.1.2}$$

Additionally, the velocity is related to the wavelength and frequency, f, of light as shown in Eq. 2.1.3 [2]. An examination of the electromagnetic spectrum reveals a range of frequencies from 3 Hz (AC power radio waves) to 3e24 Hz (gamma rays) with corresponding wavelengths of 1e8 m to 1e-16 m. The visible spectrum is generally characterized by wavelengths between 380 nm (violet) and 770 nm (red) [3].

$$v = \lambda f \tag{2.1.3}$$

The relationships given in Eqs. 2.1.2 and 2.1.3 allude to the wave nature of light (i.e., when speaking of the wavelength of light). However, the wave model cannot always predict the behavior of light. Light behavior is better described by a theory which incorporates both wave and particle models, generally referred to as the wave-particle duality. In some situations, the wave theory is useful to describe the behavior of light (e.g., interference) and in others the particle nature is more applicable (e.g., photoelectric effect) [3]. The theory of quantum electrodynamics (QED) incorporates the dual nature of light and successfully predicts all types of light behavior (e.g., diffraction, reflection, refraction, partial reflection, etc.) using probability theory.

As an example, consider the simple case of reflection off a plane mirror. Let there be a very low intensity, single frequency (monochromatic) source that emits only one particle of light, or photon, at a time. This light is incident on a plane mirror with a photomultiplier positioned as shown in Figure 2.1.1 to detect any reflected photons. Only photons which actually reflect off the mirror surface will be considered (i.e., any photons which travel directly from the source to the detector will be neglected).

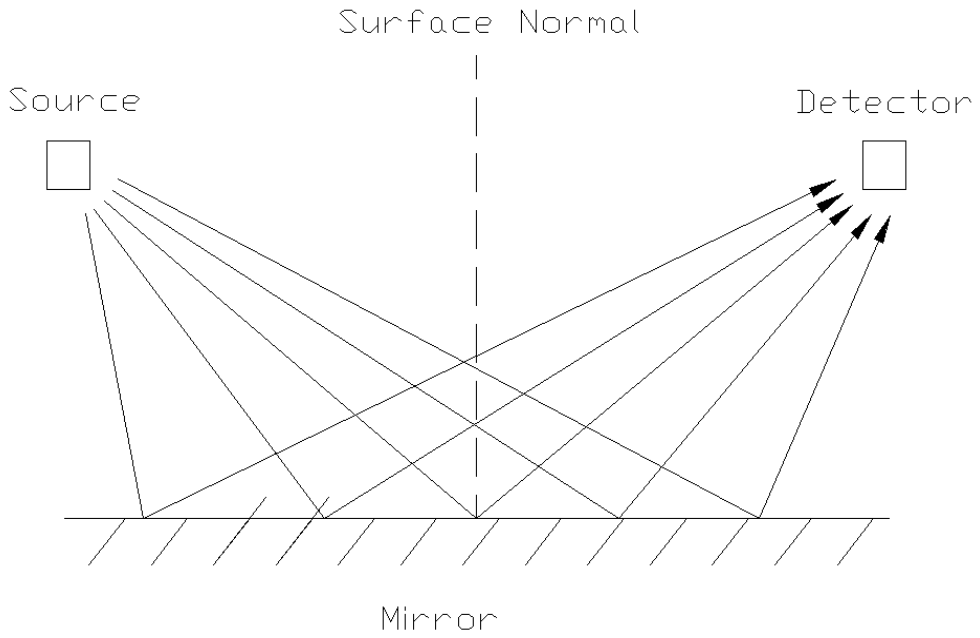

Figure 2.1.1: Plane mirror reflection.

The photons are free to travel in any path from the source to the detector, and actually do. A separate 'probability arrow' can be drawn to represent each possible path that a photon may take from the detector to the source. The length of the 'arrow' for each path represents the probability that a photon would take this particular path. The angular orientation of the 'arrow' symbolizes the time it takes for the photon to reach the detector. For example, a longer path will be represented by an 'arrow' which is rotated clockwise by several degrees (i.e., the second hand on a stopwatch after several seconds from vertical), while the 'arrow' for a very short path would be nearly vertical (i.e., the second hand is near vertical when the count in seconds is near zero).

Since the photons have an equal probability of following any path, all arrows have equal lengths. The orientations of the individual arrows will vary, however, since the path lengths are not equal. A photon which travels straight down to the mirror and then to the detector has a longer path length than one which reflects off the mirror center. If the arrow orientations represent the time of flight, the path taken will determine the arrow direction. The implementation of vector addition to sum the individual arrows from all possible paths gives a large resultant arrow. The length of the arrow is the probability amplitude and a long arrow implies an event is likely to occur. Therefore, QED predicts light will indeed reflect off the mirror. Furthermore, the magnitude of the resultant arrow

is most strongly influenced by the arrows which represent paths near the middle of the mirror. Since paths near the center of the mirror take approximately the same time and, therefore, have basically the same orientation, it is these paths of least distance (and time) that most affect the final arrow length and high probability of reflection. Therefore, the assumption that light travels in paths of least time (i.e., the law of reflection which states that the incident angle equals reflected angle) is an acceptable approximation, although not an exact picture of light behavior [4].

2.2 Polarization

Light can be described as a transverse electromagnetic wave with fluctuating electric, **E**, and magnetic, **B**, fields which are mutually perpendicular to one another, as well as the direction of propagation of the wave. The polarization of the wave is defined, by convention, as the direction of the electric field vector (since this is the more easily measurable quantity). If this vector lies in a plane for all temporal and spatial positions, the light is said to be linearly polarized.

Randomly polarized (or unpolarized) light, on the other hand, has an **E** vector which does not lie in a single plane and does not vary spatially in a repeatable manner. This unpolarized light, such as sunlight or the light emitted by a hot filament, may be linearly polarized by passing the light through a Polaroid™, or polarizing filter. This dichroic material, originally developed by E. H. Land, allows one polarization component (e.g., the vertical) to pass through and absorbs all others. The transmission axis (the vertical axis in this example) is defined as the direction in the material which suppresses vibrations and, therefore, absorbs little of the light energy. The direction orthogonal to the transmission axis blocks the light polarized in this direction by allowing the material electrons to vibrate when excited by the light, thereby absorbing the light energy. Figure 2.2.1 represents the case of absorbing horizontal polarizations and transmitting the vertical. Other methods of producing polarized light include reflection, scattering and birefringence [3].

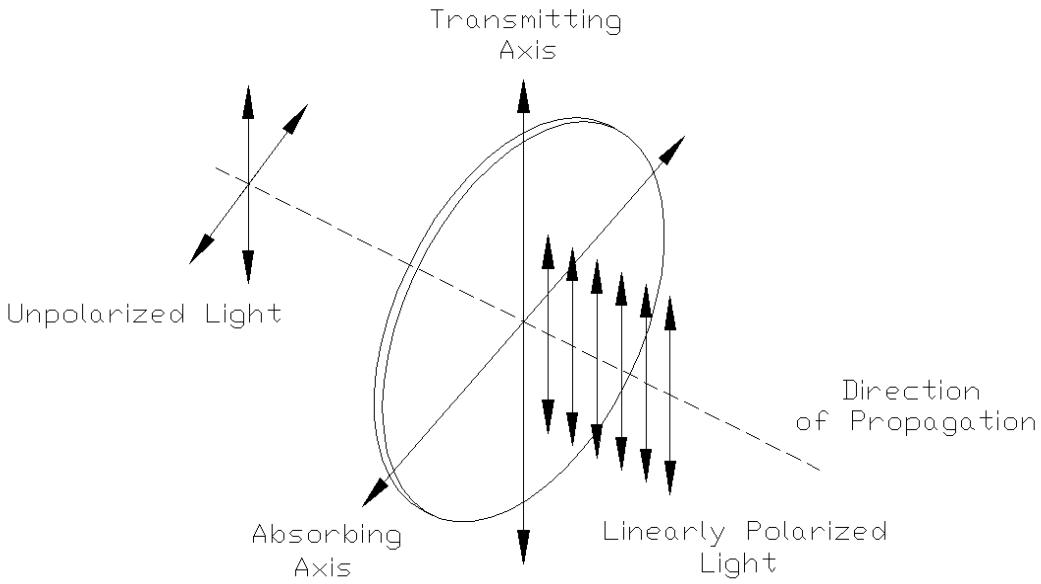

Figure 2.2.1: Polarizing filter.

The reader may be aware that quality sunglasses have lenses made of dichroic polarizing material. Light reflected from a horizontal surface, such as the highway, has a polarization state which is mostly linearly polarized in the horizontal plane. The lenses, with a vertical polarization axis, almost completely absorb the horizontal orientation and substantially reduce glare.

Next, consider two, equal magnitude waves with perpendicular polarizations (electric field vectors $\mathbf{E_1}$ and $\mathbf{E_2}$ perpendicular) and identical directions of propagation. If these two waves are in phase, the resultant polarization, found by the vector addition of $\mathbf{E_1}$ and $\mathbf{E_2}$, will lie in a plane oriented at 45° with respect to each of the original $\mathbf{E}$ fields. This is also termed linearly polarized light and is shown in Figure 2.2.2.

If these two, equal magnitude waves are now shifted in phase by 90° relative to one another, the resultant vector no longer lies in a single plane. Instead, it traces out a helical path along the direction of propagation. This situation is defined as circular polarization. The electromagnetic wave is termed right circularly polarized if the helical path is clockwise as one looks *back* along the direction of propagation and left circularly

polarized if the direction is counter-clockwise. Figure 2.2.3 shows an example of left circular polarization. Viewed head-on, the polarization vector traces out the Lissajous figure of resultant electromagnetic field vibration [3]. In this case, the figure is a circle. In the more general case, when the phase shift is neither 0° or 90° (or an integer multiple) or the magnitudes of the two electric field magnitudes are not equal, the polarization is defined as elliptical. In this instance, the polarization vector traces an elliptical path along the direction of propagation (i.e., the Lissajous figure is an ellipse). Depending on the phase difference, the tip of the resultant electric field vector may trace clockwise or counter-clockwise paths.

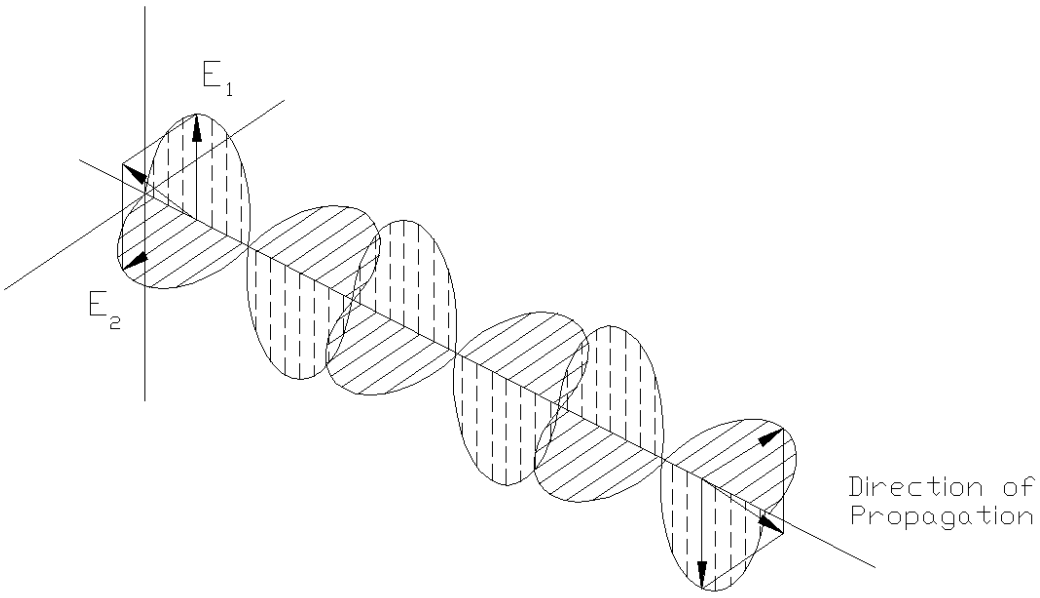

Figure 2.2.2: Linearly polarized light.

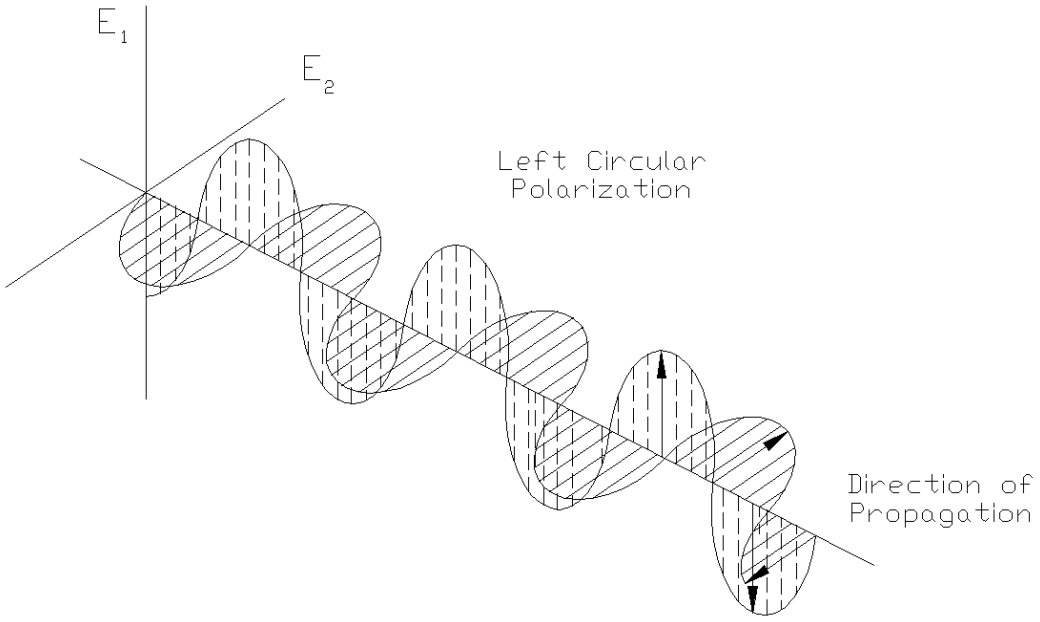

Figure 2.2.3: Left circularly polarized light.

In many situations, it is desired to change the polarization of light by shifting one of the two waves with orthogonal electric field vectors relative to the other, as described previously. A birefringent material is particularly useful in this instance. Birefringent materials exhibit a dependence of the index of refraction on the direction of polarization of the incident electromagnetic wave. Notice from Eq. 2.1.1 that a higher refractive index yields a slower velocity of propagation in the given material. Therefore, when the two waves with perpendicular polarization enter the material (with the optical axis parallel to one polarization), one wave will travel slower than the other (due to a higher n) and introduce some phase shift between the two on exit from the material.

In order to convert linearly polarized light to circular polarized (or vice versa), a 90° phase shift must be introduced in one axis relative to the other. The name for the birefringent optic which completes this conversion, a quarter-wave plate (or quarter-wave phase retarder), is derived from the ¼ cycle delay which results from this 90° phase shift. The quarter-wave plate has defined two optical axes, which are mutually orthogonal. The slow axis introduces a 90° phase shift (due to a higher index of refraction) in the light which travels along this direction relative to light which propagates along the fast axis.

As a final word in this brief outline of polarization, it should be noted that an elegant representation of the polarization of electromagnetic waves is given by the Jones vector notation. The Jones vector is a 2x1 column vector which denotes the polarization state of a wave using real and imaginary values. Also, the polarizing elements described previously may be modeled by 2x2 matrices. The matrix pre-multiplication of the Jones vector by the matrices of the polarizing elements which act on the wave gives the final polarization state of the original wave. The reader is referred to [3] for more information on this topic.

2.3 Interference

The basis for interferometry is the interference of two or more electromagnetic waves in space. The magnitude of the resultant electric field is defined by the principle of linear superposition [2]. When two coherent (constant initial phase), non-orthogonal waves (for simplicity, assume identical polarizations) arrive at the same point, their phase relationship determines the final magnitude. Constructive interference occurs when the waves are in phase and gives a total magnitude equal to the sum of the individual magnitudes. Destructive interference takes place when the waves are 180° out of phase. The resultant amplitude is the difference between the two individual amplitudes. For equal initial amplitudes, this gives total cancellation.

A popular example of this two source interference is shown in Figure 2.3.1. In this experiment, first performed by Thomas Young in 1802, a coherent monochromatic source is incident on two narrow slits in a screen. This source is typically taken to be a point source which has wavefronts, or loci of points with the same phase, which are ideally spherical in shape. The two light paths which show through the two narrow (ideally point source) slits also exhibit coherent spherical wave fronts. A screen placed in the path of these two waves shows alternating bright and dark bands. This is an interference pattern which demonstrates both constructive (bright bands) and destructive (dark bands) interference between the light waves emitted from the two slits.

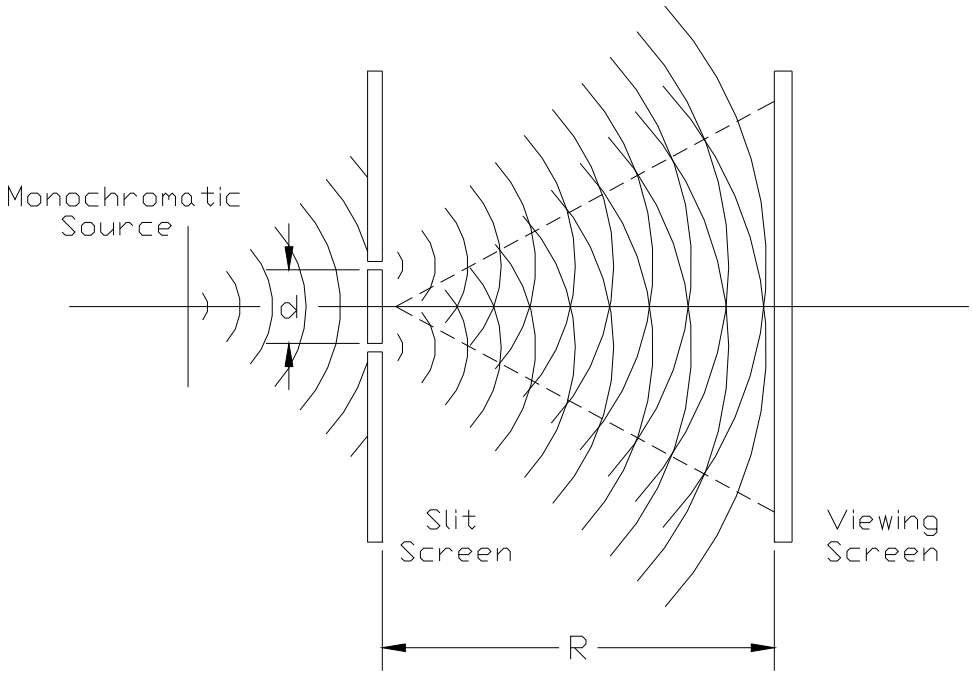

Figure 2.3.1: Young's double slit experiment.

The monochromatic wavelength of the source may then be calculated, according to Eq. 2.3.1, by measuring the distance between the slits, d, the distance between the viewing screen and the slits, R, and the distance between adjacent bright band centers, δ.
For completeness, it should be noted that the effects of diffraction (also an interference phenomenon), or bending of the light waves around the slit of finite width in the screen, have been neglected in this simple analysis.

$$\lambda = d\,\delta / R \qquad (2.3.1)$$

The first displacement measuring interferometer was developed by Albert Michelson in 1881 [3]. In this experiment, light was incident on a partially silvered mirror or beam splitter (glass with a thin silver coating). This beam splitter allowed some of the light to pass through and reflected the rest. The reflected portion of the light traveled to a moveable mirror mounted on a fine pitch micrometer. The transmitted light passed through a second glass plate with the same thickness as the beam splitter to a fixed, reference mirror. The second plate, or compensator plate, was necessary to ensure that both the reflected and transmitted light traveled through an equal distance in glass, referred to as the optical path length (OPL). When the mirror mounted on the micrometer was translated relative to the fixed mirror (without changing its angular orientation), light to dark (uniform intensity) transitions due to constructive and destructive interference were seen once the beams had recombined at the beam splitter, as shown in Figure 2.3.2. A relative displacement of one-half the wavelength of the source light (λ\2) produced a light-dark-light transition, or fringe, at the viewing position. A light-dark-light transition occurred for a 360° (one wavelength) phase shift between the electric fields of the two waves [1]. This corresponded to the half-wave displacement of the mirror since the reflected wave must travel both to and from the mirror and therefore has an overall motion of one wavelength.

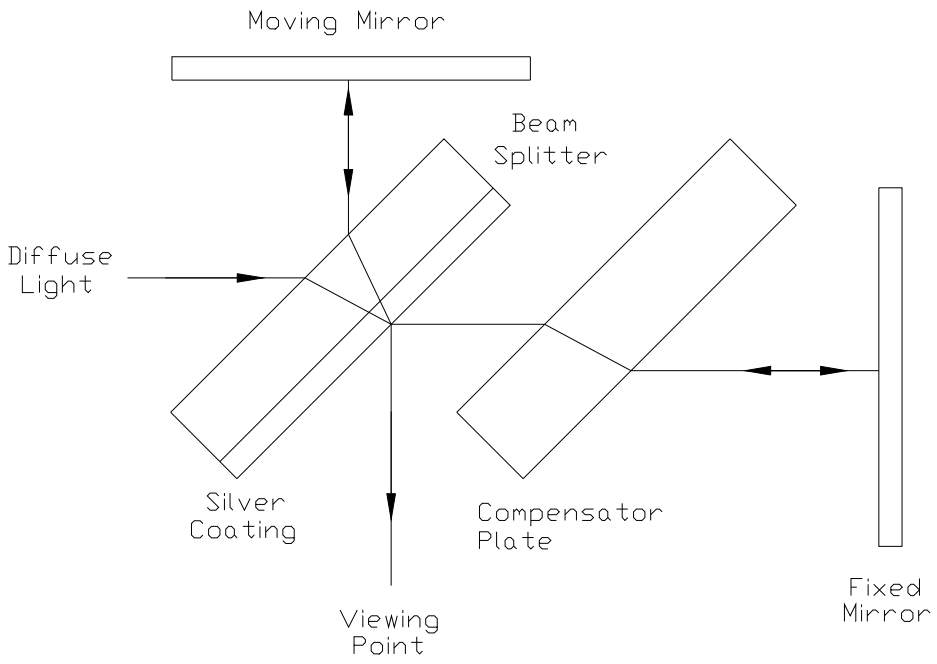

Figure 2.3.2: Michelson interferometer.

Two common variations of the Michelson interferometer are the Twymann-Green and Mach-Zehnder interferometers. The Twymann-Green, shown in Figure 2.3.3, uses a coherent point source rather than the extended source of the Michelson. The coherent source allows for unequal path lengths in the two legs of the interferometer. For this reason, the Twymann-Green interferometer is also called a Laser Unequal Path Interferometer (LUPI) [5]. Collimating lenses are used to convert the diverging rays of the point source to (essentially) parallel rays within the interferometer. The rest of the interferometer operation is analogous. The Twymann-Green interferometer is typically used to measure imperfections within other optics, provided the optics within the interferometer are high quality, by placing the optic to be measured within one of the measurement paths. The optic distorts the normally planar wavefronts by slowing the light which passes through. Interference fringes can be seen at the interferometer output due to variations in the index of refraction across the optic face. The shape of these fringes indicates where the index of refraction is constant. Therefore, the fringe shapes

can be thought of as a contour map which shows the variation of the light path length through the optic and may be used to polish the glass to a particular shape [6].

The Mach-Zehnder, shown in Figure 2.3.4, has two beam splitters and two mirrors arranged in a rectangular pattern. Typically, one path is disturbed while the other remains fixed to measure the relative change in path length.

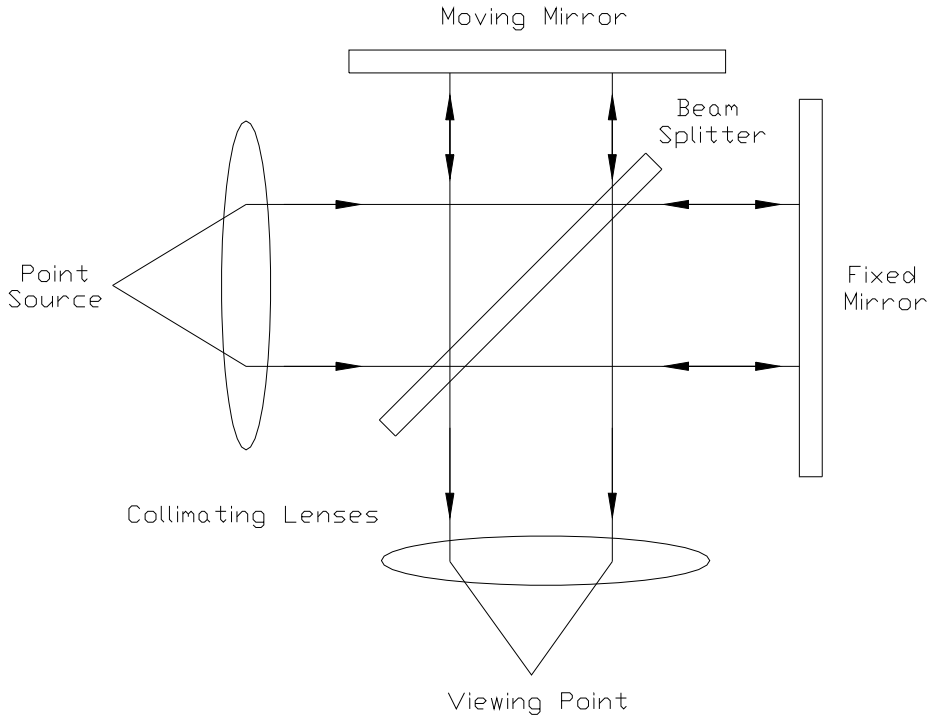

Figure 2.3.3: Twymann-Green interferometer.

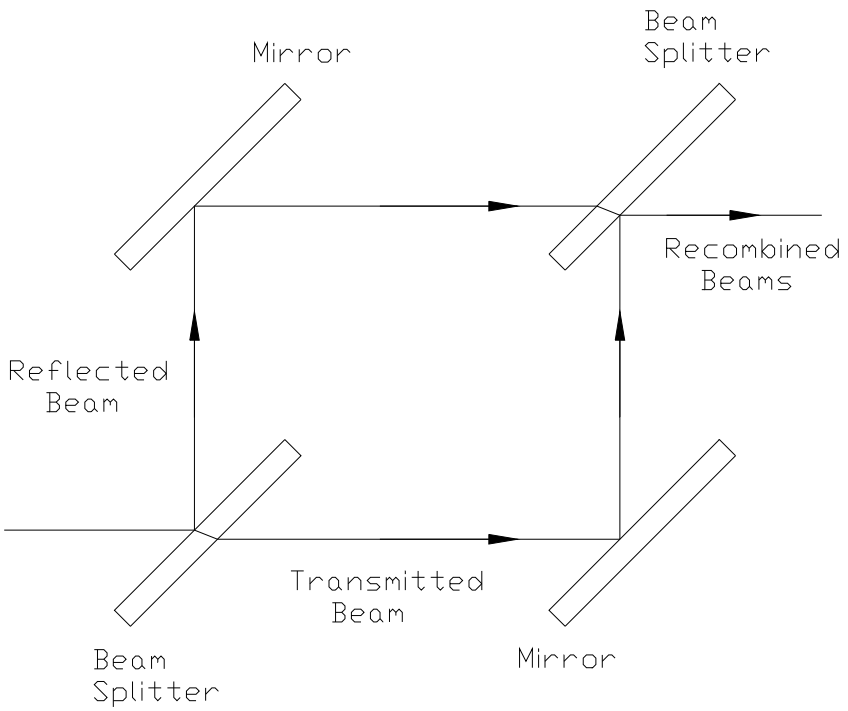

Figure 2.3.4: Mach-Zehnder interferometer.

The light-dark transitions in the Michelson interferometer discussed previously form the foundation for homodyne (DC), or single frequency, interferometry. After the two beams travel the measurement and reference paths, respectively, they must interfere. As noted, interference only occurs for beams with the same polarization state. If initially the two beams each have planar polarization perpendicular to one another, a Polaroid™ may be placed in the path, oriented at 45° to each. A portion of each wave is absorbed by the Polaroid™ and a portion passes through, each with the same polarization and now interfered. To find the total relative displacement of the moving mirror, the recombined beams are first incident on a photodetector. The photodetector then produces a signal proportional to the light intensity. For a λ\4 motion of the moving mirror, the signal will vary from the maximum value to ideally zero (one-half fringe), assuming the fixed and moving mirrors initially had an equal path length. (The resolution may be increased by adding electronic circuitry to interpolate between the light and dark conditions.) The displacement is calculated by multiplying the number of fringes by ½ (the scale factor for a single pass Michelson interterometer).

The measurement signal in a DC interferometer is therefore a function of the photodetector output amplitude. Several problems may arise from this reality. First, the system is susceptible to variations in the source intensity and ambient light since the measurement amplitude will vary for no motion. Second, a loss of the beam from either leg (or both) cannot be distinguished from total destructive interference. Finally, if motion is stopped at a maximum, there is no directional knowledge when motion starts again since either direction will give the same reduction in photodetector output. To obtain directional knowledge, part of the interfered signal can be split off, directed through a quarter wave plate to shift the signal by 90° and compared to the original signal. This is analogous to the quadrature detection used in rotary encoders.

To this point, the interference of the two waves (recombined at the beam splitter) which provides uniform illumination at the photodetector has been taken for granted. If the two beams are not precisely parallel (mirrors are not perfectly orthogonal), fringes of equal spacing will be seen at the photodetector rather than the desired uniform intensity [3]. These fringes appear as dark bands across the otherwise bright output. As one mirror moves relative to the other, the fringes translate, but do not change the total intensity incident on the photodetector. Therefore, no motion is observed. A simple proof of this concept is to superimpose two transparent plastic sheets, each with finely spaced lines printed on one side. If the lines are not perfectly parallel when the sheets are placed over one another, fringes will be seen which move across the sheets during relative motion. If the lines on the two sheets are perfectly parallel, however, uniform intensity (bright and dark) will be seen for relative motion.

In reality, the alignment of the mirrors in the Michelson interferometer is challenging and time-consuming. It requires precise, high resolution angular adjustments of the mirrors and a stable optical bench to maintain the alignment. The minimum required alignment accuracy can be quantified according to Figure 2.3.5. As an example, consider two 3 mm diameter beams of green (coherent) laser light with perfectly planar wavefronts and equal wavelengths of 510 nm. As shown in Figure 2.3.5, the maximum allowable misalignment occurs when the edge of wavefront #2a overlaps with wavefront #1b. For the typical values given, this predicts a maximum misalignment, α, of 35.07 arc-sec. See Equation 2.3.2.

$$\alpha = \tan^{-1}(\lambda / D) * 3600 \text{ arc-sec}, \quad \text{where } \lambda = 510\text{x}10^{-9} \text{ m and } D = 3\text{x}10^{-3} \text{ m} \qquad (2.3.2)$$

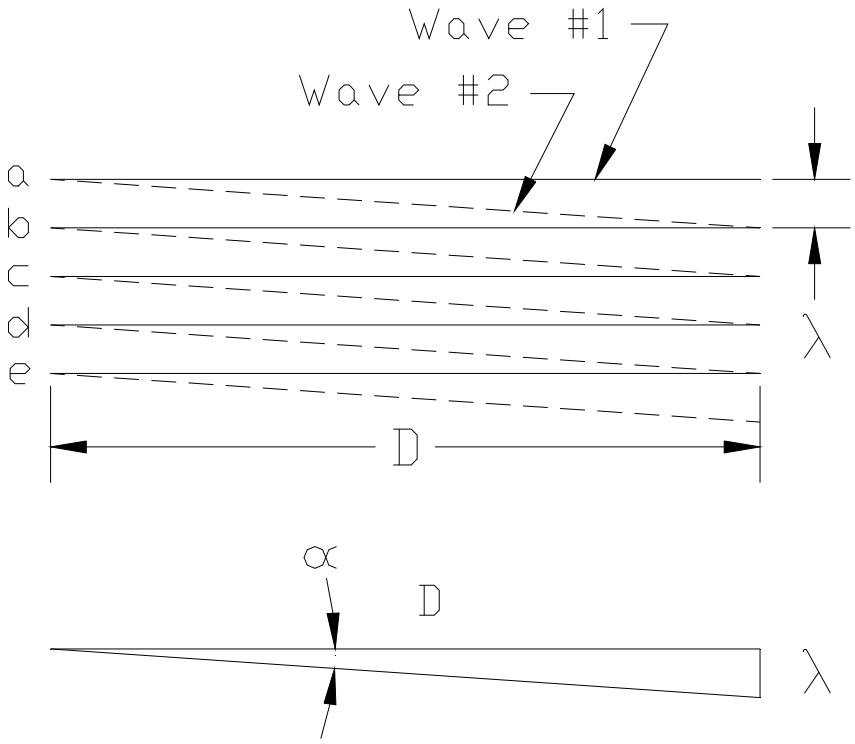

Figure 2.3.5: Alignment accuracy.

2.4 Heterodyne Interferometry

Modern users of linear displacement measuring interferometers rely mainly on heterodyne (AC), or two frequency, interferometry. The light source is, in most instances, a frequency-stabilized Helium-Neon (He-Ne) laser tube with some method of generating a second frequency (within the bandwidth of modern electronics) from the natural He-Ne center frequency (roughly 474e3 GHz) within the laser head.

Several longitudinal modes may actually be available within the single TEM_{00} transverse mode of light emitted from the laser head, depending on the length of the lasing cavity. However, the frequency split between modes is normally hundreds of megahertz and beyond the bandwidth of most modern electronics. These adjacent longitudinal modes each satisfy the resonant condition for lasing, which is dependent on both the laser cavity length and the wavelength of light, at different frequencies under the He-Ne gain curve. See Eq. 2.4.1. Furthermore, the physics of the process requires that adjacent modes be orthogonally polarized. The frequency difference between two longitudinal modes may be calculated according to Eq. 2.4.2 [12]. The TEM_{00} transverse mode has a Gaussian cross-sectional intensity profile. The variation in irradiance across the beam is given in Eq. 2.4.3 [3].

$$2L = m\lambda, \qquad \text{where } L = \text{laser cavity length} \tag{2.4.1}$$

m = integer longitudinal mode number
λ = light wavelength

$$f_{m+1} - f_m = \frac{c}{2Ln}, \qquad \text{where } f_i = \text{light frequency} \tag{2.4.2}$$

c = speed of light
n = refractive index of medium

$$I = e^{\frac{-8y^2}{D^2}}, \qquad \text{where } I = \text{beam intensity} \tag{2.4.3}$$

y = transverse beam direction
D = beam width at given position

In heterodyne systems, by definition, the frequencies of the measurement and reference beams differ slightly. When these two beams of different frequency are recombined at the beam splitter (after traveling different paths) and passed through a Polaroid™, rather than pure constructive or destructive interference, linear superposition yields a wave with a periodically varying amplitude and some phase as shown in Figure 2.4.1.

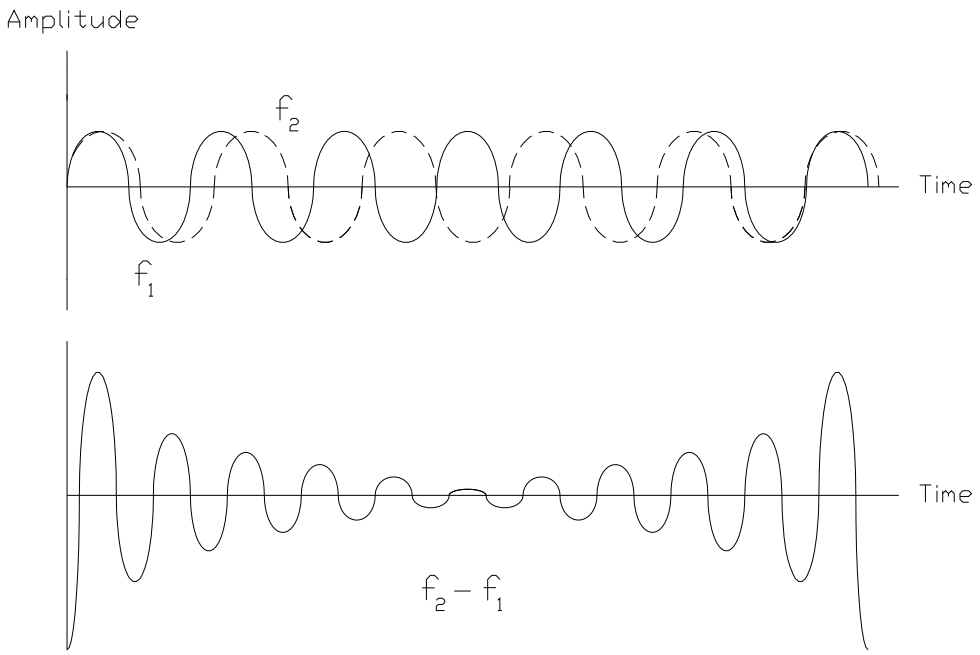

Figure 2.4.1: Beat phenomenon.

If the two beam frequencies are considered as phasors (or vectors) rotating with unequal angular velocities, the phasor with the higher frequency will periodically overtake the slower phasor and the two will have a relative angular velocity of 2π (f_1 - f_2) radians/second. The time (in seconds) it takes for one phasor to overtake the other is (f_1 - f_2)$^{-1}$. If the two phasors are equal in amplitude (A) and have a small difference in frequency, the resultant motion, y, is described by Eq. 2.4.4. This is essentially a sine wave with a slowly varying, or modulated, amplitude (given by the cosine term). The frequency of the varying amplitude envelope, or beat frequency, is equal to the difference between the two individual frequencies of the measurement and reference beams, (f_1 - f_2) in Hz. The frequency of the actual waveform is the average of the two original signal frequencies, 0.5 (f_1 + f_2) [7][8].

$$y = A \sin \omega_1 t + A \sin \omega_2 t \qquad (2.4.4)$$
$$= 2A \cos ((\omega_1 - \omega_2)/2)t * \sin ((\omega_1 + \omega_2)/2)t$$

This heterodyne technique carries the displacement information in the phase of the interfered measurement and reference signals rather than the amplitude. In the frequency domain, a motion of the moving retroreflector causes a change in frequency of the beat signal due to the Doppler shift. For a perfectly sinusoidal beat signal, the single Fourier transform spike at the beat frequency can be viewed sliding left or right (depending on the displacement direction) using a spectrum analyzer. In this way, the frequency/phase relationship can be considered analogous to the velocity/position relationship, where the frequency is simply the circular velocity.

The measurement and reference beams can therefore be represented by phasors (or vectors) which are rotating with an angular velocity equal to the frequency of the light. The measurement phasor will either lead or lag the reference phase depending on the direction of the moving mirror (and subsequent Doppler frequency shift). The amount of lead or lag represents the phase between the measurement and reference beams. Using phase measuring electronics, the instantaneous phase between the two phasors is recorded and converted to displacement. See Figure 2.4.2. In the time domain, the beat frequency sinusoid can be seen translating in either direction on an oscilloscope. The amount of shift is the phase change, which carries the displacement information.

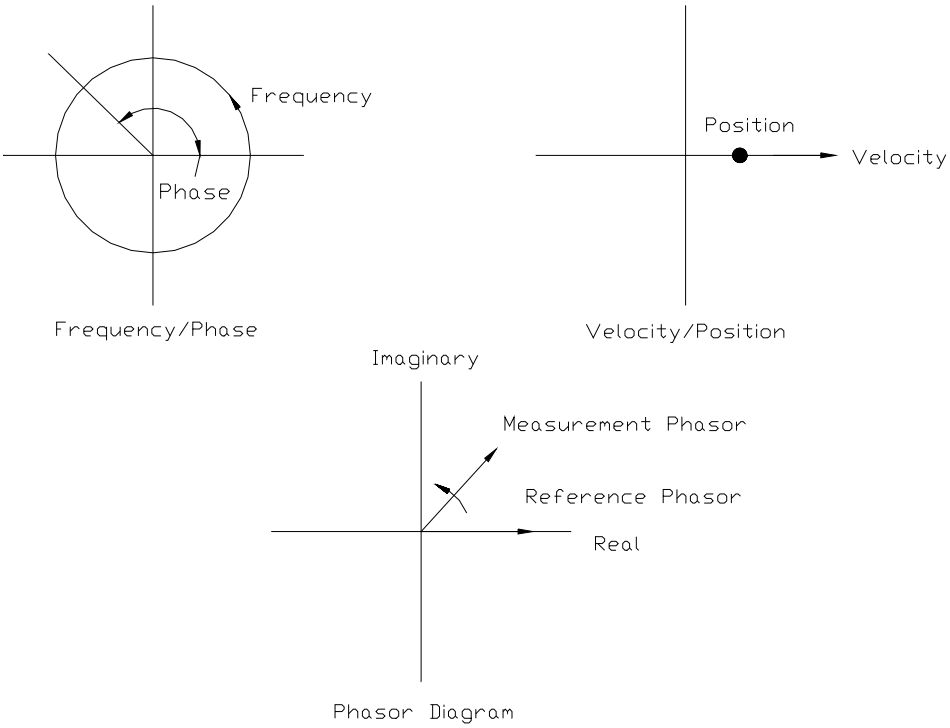

Figure 2.4.2: Heterodyne phase relationships.

The Doppler shift, which is responsible for the phase change in the interfered signals, can be explained in several ways. One can characterize the shift by the time of flight, such as the change in pitch observed when a car with the horn blowing passes by or Doppler radar. It is also possible to think of the light as being *stretched* by the velocity of the moving reflector [7].

An intuitive explanation is to consider the light path as a pipeline [9]. The wavelengths, λ, can then be thought of as filling up the pipeline. For a wavelength of 632.8 nm (He-Ne light), this gives a wavenumber or V-number, λ^{-1}, of 1580278.1 m^{-1}. The wavenumber represents the number of λs in one meter of this imaginary pipeline. If the pipeline now begins lengthening at 1 m/s, there will be 1580278.1 more λs entering the pipeline than exiting. This is analogous to moving the mirror away from the beam splitter in the Michelson interferometer, except that this number is doubled because the light must travel both to and from the mirror (this represents a fold factor of` 2 or scale factor of

1/2). Therefore, a negative frequency shift in the beat frequency of 2*1580278.1 Hz/m/s will be seen for this motion direction because there is a deficit of λs.

To further clarify the Doppler shift concept, the author would also like to add the notion of a 'bag of light', or λs, attached to the end of the pipeline. As the pipeline is lengthening, the 'bag of λs' is emptying and the deficit describes the negative frequency shift previously noted.

Now consider the mirror moving toward the beam splitter. In this case, the pipeline will be shrinking at 1 m/s and there will be 1580278.1 more λs exiting the pipeline than entering (i.e., the 'bag of λs' is filling). Now the frequency shift will be positive 2*1580278.1 Hz/m/s for the interferometer. This number gives a general rule of thumb for the frequency shift of red He-Ne laser light in a single-pass Michelson interferometer. The shift for a velocity of 1 ft/s is roughly 1 MHz (or 1 MHz/ft/s). [The actual value is 0.9633375 MHz/ft/s.]

In modern heterodyne interferometry, however, the situation is a little more complex. The Doppler shifted frequency is the difference between the optical frequency (474e12 Hz for He-Ne), designated f_o, and the second frequency, $f_o \pm f_s$, normally generated within the laser head by either acousto-optic modulation or Zeeman split. This second frequency can be upshifted or downshifted by the amount f_s. In this case, consider an upshifted second frequency of $f_o + f_s$.

For no motion, the beat frequency is the difference between the frequencies of these two signals, or $f_s = ((f_o + f_s) - f_o)$. Either the optical or shifted frequency signal could function as the reference beam, so either may be Doppler shifted (by retroreflector motion). For instance, if the f_o mirror was moving away from the beam splitter, this signal would be Doppler shifted down by an amount f_d. According to Figure 2.4.3, this would produce an increase in the beat frequency and a positive phase (and therefore displacement) since the total difference between the two signals is increasing. Moving the $f_o + f_s$ mirror in the same direction will have the opposite effect.

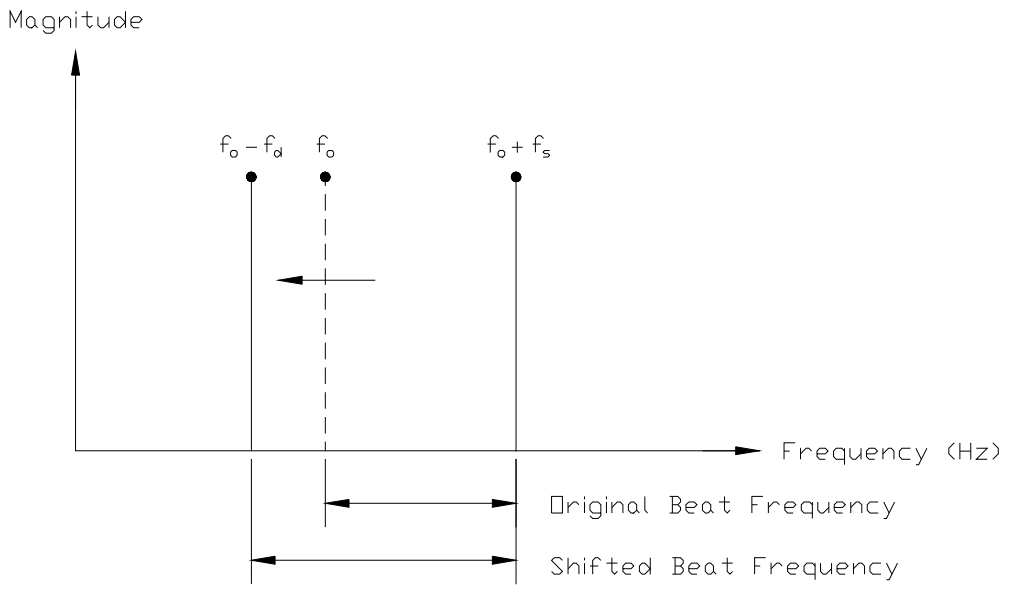

Figure 2.4.3: Beat frequency shift.

A brief description of two common methods to generate the second, shifted frequency for use in heterodyne systems will now be provided (recall that the naturally available adjacent longitudinal modes are separated by hundreds of megahertz and the frequency split is generally outside the electronics' bandwidth). In the acousto-optic technique, a single longitudinal mode (of the TEM_{00} transverse wave) is passed through an acousto-optic modulator. This device is, in its simplest form, a piece of glass with a PZT attached to one edge. This transducer is driven at the shifting frequency by a stable quartz oscillator and produces a traveling acoustic (sound) wave in the glass. This traveling sound wave produces successive compressions and rarefractions in the medium which changes the index of refraction periodically along its length. The periodically varying refractive index produces a moving diffraction grating. When linearly polarized, monochromatic light is incident on this phase diffraction grating at the Bragg angle, θ_B, a large portion of the beam is diffracted and frequency shifted (for certain crystals the polarization vector is also rotated by 90°), while the rest is transmitted (with no frequency shift). See Figure 2.4.4. The diffracted and transmitted waves are diverging at twice the Bragg angle and are, therefore, spatially separated. The Bragg angle, which is

proportional to the driving frequency, $f_{acoustic}$, is given in Equation 2.4.5. The two frequencies may then be recombined into a single heterodyne beam.

$$2\,\theta_B = \lambda \setminus \lambda_{acoustic}, \qquad \text{where } \lambda_{acoustic} = V_{acoustic} / f_{acoustic} \qquad (2.4.5)$$
$$V_{acoustic} = \text{acoustic velocity}$$

The Zeeman frequency split is accomplished by placing a magnetic field around the He-Ne laser tube. At low magnetic power, there exists one (preferential) linearly polarized, longitudinal mode in the laser tube (provided the laser cavity is "short"). At some higher power level, this single mode snaps into two circularly polarized modes (one left, one right) of different frequencies. The actual frequency difference between the two modes is dependent on the magnetic field strength. The He-Ne medium is able to support the two modes of different wavelengths (which are not harmonics of one another) in one tube due to the presence of a circular birefringence [9]. See Figure 2.4.5 [1]. In other words, the two modes see effectively different laser cavity lengths, due to the different indices of refraction, and satisfy the condition for lasing (Eq. 2.4.1) at two different wavelengths (frequencies).

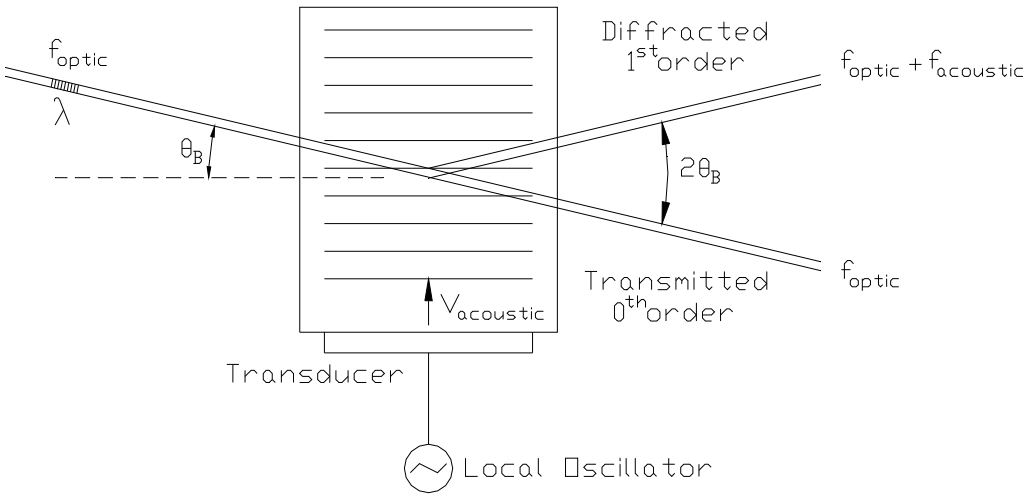

Figure 2.4.4: Acousto-optic modulator.

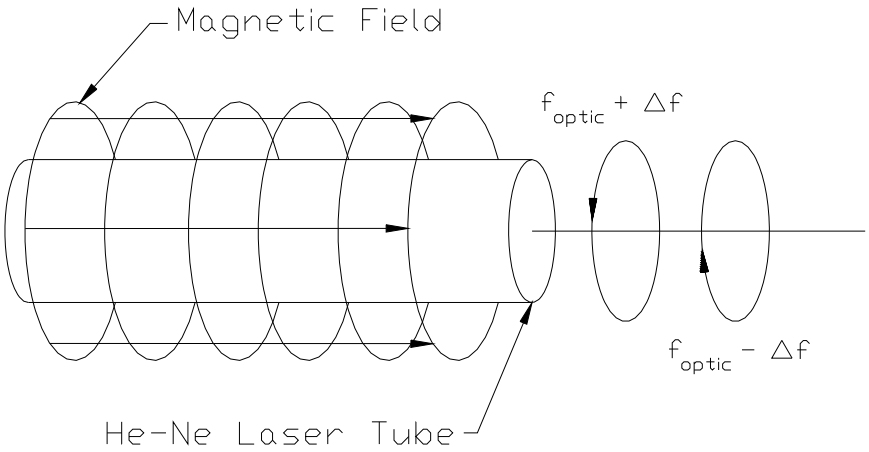

Figure 2.4.5: Zeeman split.

The mathematics behind the heterodyne interference will now be discussed. The math is not complex and relies simply on the trigonometric relationship 2 cos(A) cos (B) = cos (A+B) + cos (A-B). The electric field, **E**, of the resultant beam after interference of the measurement (moving mirror) and reference beams (fixed mirror) is expressed in Eq. 2.4.6. Again, the interference of the two beams with initially perpendicular planar polarizations is accomplished using a 45° Polaroid™. The subscript 'm' refers to the measurement beam and the subscript 'r' to the reference beam.

$$\mathbf{E} = E_m \cos((\omega_o + \omega_s)t + \phi_o + \phi_d) + E_r \cos(\omega_o t + \phi_o), \qquad (2.4.6)$$

where E_m, E_r = magnitude (V/m)
ω_o = optical frequency (rad/s)
ω_s = shift frequency (rad/s)
ϕ_o = initial phase (rad)
ϕ_d = Doppler phase shift (rad)

When the interfered beam in incident on a photodetector, the output is proportional to the field strength squared ($i \sim E^2$). The quantity $\mathbf{E}^2$ and resultant simplifications are shown in Eq. 2.4.7. The final simplification step is the detector output because all frequencies except ω_s are outside the detector's bandwidth (i.e., the detector acts like a low pass filter) and the DC component is not used in the dynamic, heterodyne measurement.

$$E^2 = E_m^2 \cos^2((\omega_o + \omega_s)t + \phi_o + \phi_d) + E_r^2 \cos^2(\omega_o t + \phi_o) + 2 E_m E_r \cos((\omega_o + \omega_s)t + \phi_o + \phi_d) \cos(\omega_o t + \phi_o) \quad (2.4.7)$$

Expand to obtain:

$$= 0.5 E_m^2 (\cos(2(\omega_o + \omega_s)t + 2\phi_o + 2\phi_d) + \cos(0)) + 0.5 E_r^2 (\cos(2\omega_o t + 2\phi_o) + \cos(0)) + 2 E_m E_r (0.5 (\cos(2\omega_o t + \omega_s t + 2\phi_o + \phi_d) + \cos(\omega_s t + \phi_d)))$$

Ignore all terms which contain the optical frequency (outside detector bandwidth):

$$= 0.5E_m^2 + 0.5E_r^2 + E_m E_r \cos(\omega_s t + \phi_d)$$

Neglect the DC components of the signal:

$$= E_m E_r \cos(\omega_s t + \phi_d)$$

A typical linear interferometer consists minimally of a two-frequency He-Ne laser head with the two frequencies occupying perpendicular polarizations (polarization coded), a polarization beam splitter, two retroreflectors and a heterodyne receiver with the necessary phase measuring electronics. Variations in the optical setup allow measurement of linear and angular displacement, straightness of travel, flatness, squareness and parallelism, as well as changes in the refractive index of air (although all are derived from a change in displacement) [1].

Simple linear displacement is measured as shown in Figure 2.4.6. At the polarization beam splitter it can be seen that the polarization parallel to the plane of incidence is transmitted, while the vertical polarization is reflected. The polarization parallel to the plane of incidence (the plane of the page) is normally referred to as the transverse magnetic (TM) mode, or 'p' mode. The polarization perpendicular to the plane of

incidence is called the transverse electric (TE) mode, or ‘s’ mode [3]. Either path can act as the reference or measurement leg of the Michelson interferometer. The beams are recombined (for interference) when they return from their respective retroreflectors. The retroreflectors, glass optics with three silvered faces containing a solid right angle, simplify the alignment procedure greatly by returning a beam parallel to the incident beam (after three reflections) regardless of the incident angle [6]. This nearly guarantees interference provided there are no significant changes in the wavefront shape of the transmitted and reflected beams. Figure 2.4.7 shows a method of measuring angular deviations using only a polarization beam splitter (PBS), a 90° prism and two retroreflectors.

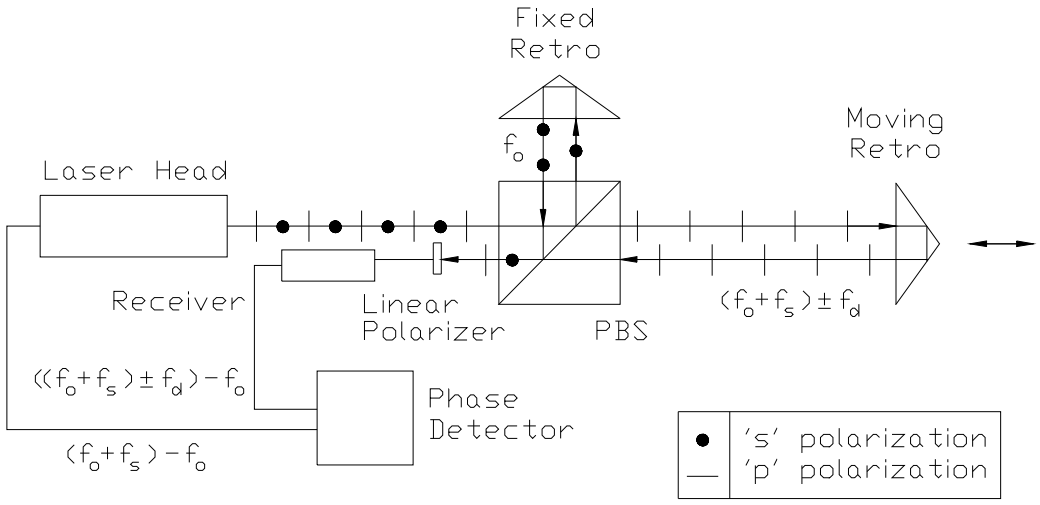

Figure 2.4.6: Linear displacement interferometer.

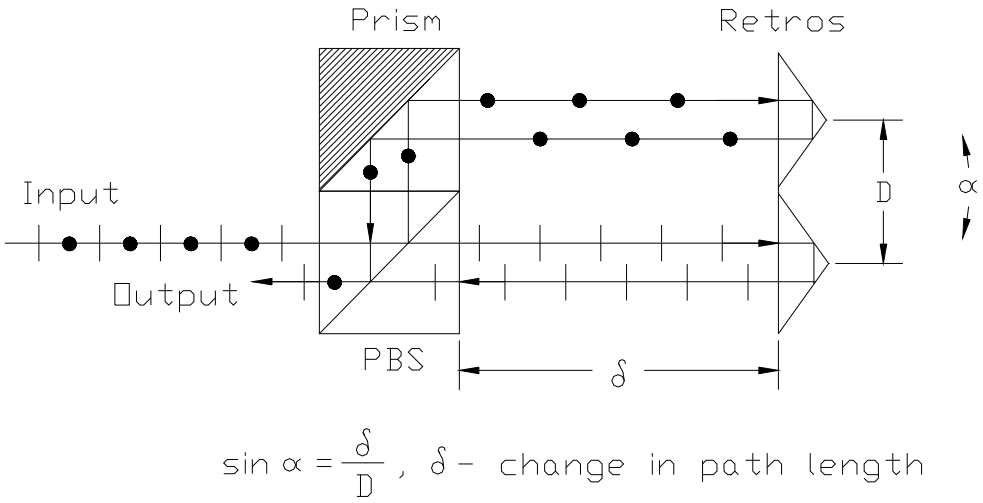

Figure 2.4.7: Angular measurement setup.

2.5 Fiber Optics in Interferometry

A discussion of modern heterodyne interferometry would be remiss if a brief description of fiber optics and their application to heterodyne interferometry were not included. Although the main use of fiber optic technology is in the field of communications, metrology applications, such as fiber optic sensors and fiber delivery/collection of heterodyne measurement signals, are becoming quite common. Heterodyne fiber delivery/collection will be discussed here.

An example heterodyne fiber delivery/collection system is shown in Figure 2.5.1. The different fiber types shown in the figure, single mode polarization maintaining (SMPM) and multimode (MM), will be discussed after a brief review of total internal reflection, launching conditions, fiber numerical aperture (NA) and mode distribution in fibers.

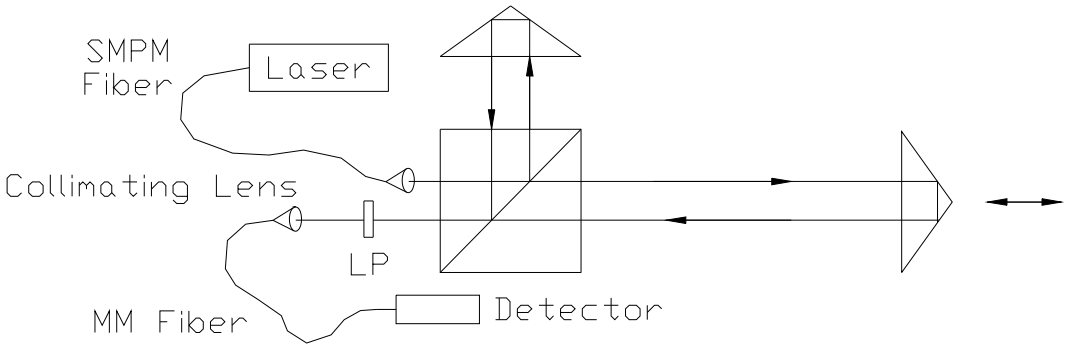

Figure 2.5.1: Fiber delivery/collection.

When light travels from one medium to a medium with a different refractive index, it obeys Snell's law of refraction. See Equation 2.5.1. In the case of light entering a medium with a lower index of refraction, n_b, the refracted angle, ϕ_b, is greater than the incident angle, ϕ_b (i.e., the light bends away from the surface normal). See Figure 2.5.2. As the incident angle is increased, the refracted angle in the second medium increases until it reaches 90°. At this point, the interface between the two mediums begins to act as a perfect mirror and the light is reflected back into the first medium according to Snell's law (incident angle equals reflected angle). This situation is called total internal reflection (TIR). The critical angle of incidence for TIR may be derived from Snell's law by substituting 90° for the refracted angle. The critical angle, $\phi_{critical}$, is given in Eq. 2.5.2. If the first medium is a transparent rod, or fiber optic, and the surrounding medium is air (or any medium with a lower refractive index), light input at the critical angle will be trapped within the rod by TIR [2].

$$n_a \sin \phi_a = n_b \sin \phi_b \tag{2.5.1}$$

$$\phi_{critical} = n_b / n_a \tag{2.5.2}$$

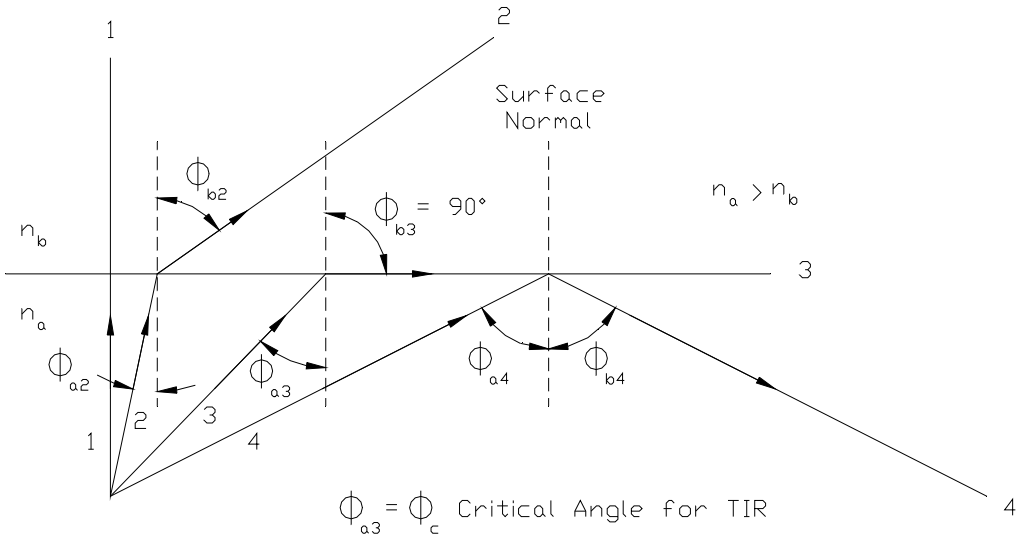

Figure 2.5.2: Total internal reflection.

The light trapped by TIR in the fiber will only remain in the fiber provided it does not come into contact with another surface. If the fiber touches a surface with a higher index of refraction, TIR will no longer occur. To circumvent this problem, fiber optics consist of a core, cladding and protective jacket. The core carries the light and has a higher index of refraction, n_{core}, than the cladding, $n_{cladding}$, which surrounds the core.

Two typical cross-sectional profiles for the core index of refraction are shown in Figure 2.5.3. The step index profile has an abrupt discontinuity at the cladding interface, while the graded-index profile has a smoothly changing index of refraction, typically parabolic in shape. The advantage of graded-index fiber is seen in communications. For a step index, the path length for a ray entering at the maximum angle for TIR (cone angle) is longer than the path length for one which enters along the fiber axis. This different path time (due to a constant refractive index) will smear, or broaden, a pulse (bit) of information by modal distortion and limit the data transfer rate (bandwidth). A graded-index fiber with a parabolic profile significantly reduces this problem [10]. Additionally, a reduction in the number of modes propagating in the fiber lessens the effect of modal distortion.

Material dispersion, inherent to all fiber optics, also limits the system bandwidth by pulse broadening. In any given material there is a dependence of the refractive index on the wavelength of light traveling in the medium. Since there are no completely monochromatic sources, the input light encompasses a range of wavelengths, referred to as the free spectral range (at full width half maximum). As this range of wavelengths propagates through the fiber, the information carried in the longer wavelengths travels faster than the information in the shorter wavelengths (i.e., the refractive index decreases with wavelength for normal dispersion). Therefore, the input pulse spreads in time and, in the extreme case, overlaps with the next pulse. Adjacent pulses can then no longer be distinguished and the data transfer rate is limited [3].

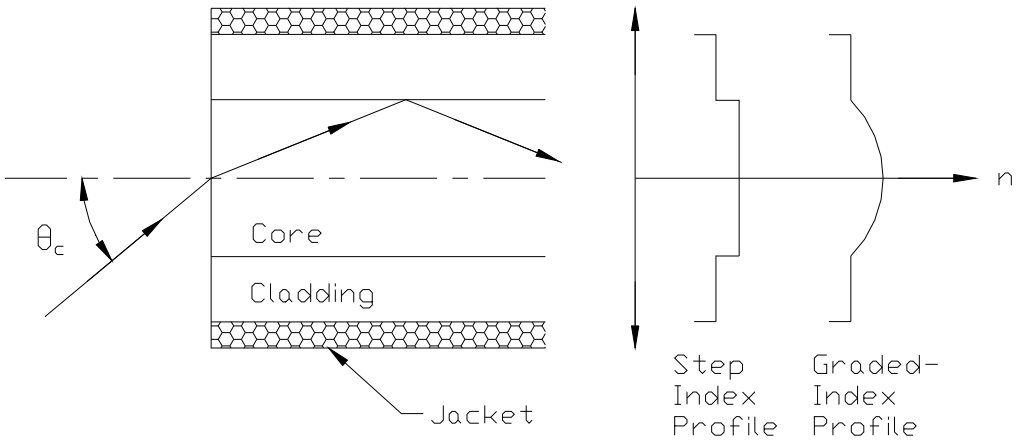

Figure 2.5.3: Refractive index profiles.

The cone of light which may be accepted by a fiber is a function of the core and cladding indices of refraction. The half-angle, θ_c, of the acceptance cone may be calculated according to Eq. 2.5.3 for a step index fiber.

$$n_i \sin\theta_c = (n_{core}^2 - n_{cladding}^2)^{0.5}, \qquad \text{where } n_i \approx 1 \text{ for light from air} \qquad (2.5.3)$$

A fiber's numerical aperture (NA), a measure of the light gathering capability of the fiber, is also a function of the core and cladding refractive indices. The NA for a step

index fiber with light incident on the fiber from air is given in Eq. 2.5.4. It should be noted that this particular figure of merit is independent of the fiber geometry.

$$NA = (n_{core}^2 - n_{cladding}^2)^{0.5} \quad (2.5.4)$$

A fiber's NA is an important consideration in the launch conditions of light into a fiber. For example, if light is introduced into the fiber with a cone of diverging rays greater than the maximum cone angle of the fiber, some of the source light cannot be propagated by the fiber. This situation is referred to as "overfilling" the fiber and causes transmission losses. If the source cone of light is less than the maximum cone angle the fiber can accept, the fiber is "underfilled", but results in less attenuation than in the overfilled case.

If light is being coupled into the fiber from a collimated source (i.e., the source emits light in only one direction), a converging (double convex) lens may be used to focus the light on the fiber core (a challenging task which is mainly a function of the angle at which the light strikes the fiber from the lens). The NA of the beam may now be found according to Eq. 2.5.5. This NA must then be compared to the fiber NA to avoid overfilling.

$$NA_{beam} = n \sin (r_o / f), \quad \text{where } r_o = \text{initial beam waist radius}, \; f = \text{lens focal length}, \; n = \text{air refractive index} (\approx 1) \quad (2.5.5)$$

Once light is coupled into the fiber, it is next important to understand how it propagates in the fiber. By combining Maxwell's equations, a wave equation may be obtained which can be solved for the distribution of the electromagnetic field across the fiber face, or the guided modes. A solution of the wave equation for these modes depends on the fiber geometry and index profile of the core and cladding. To determine the number of modes which will be supported by a given fiber, the normalized wavenumber, or V-number, may be calculated. See Eq. 2.5.6 [10]. An alternate analysis, developed in [3], suggests that the maximum number of supported modes, m_{max}, may be calculated according to Eq. 2.5.7.

$$V = k_o (a) NA, \quad \text{where } k_o = \text{free space wavenumber} = 2\pi / \lambda_o, \; a = \text{fiber core radius} \quad (2.5.6)$$

$$m_{\max} = \frac{1}{2}\left(\frac{\pi d}{\lambda_o} NA\right)^2, \qquad \text{where d = fiber core diameter} \qquad (2.5.7)$$

It can be seen that a small core diameter, small NA or a large free space wavelength, λ_o, will decrease the V-number and reduce the number of modes supported by the fiber. For V < 2.405, only a single mode (HE_{11}) will be supported. Fibers which support just this single mode are known as single mode fibers. As the V-number is increased, more modes may be carried by the fiber. These fibers are referred to as multimode fibers. Typical multimode communications fibers may have V-numbers from 50 to 150.

In many cases, it is desirable to maintain the polarization state of the input light through the length of a single mode fiber. This is the case for the fiber feed from the laser head to the interferometer (e.g., the single mode-polarization maintaining or SMPM fiber shown in Figure 2.5.1). For the fiber to maintain the input polarization state, it is stressed along a single axis to produce a birefringence in the fiber. See Figure 2.5.4 [11]. Light linearly polarized along the stressed axis travels at a slower rate than light orthogonally polarized to this axis. If the two orthogonal frequency components from the laser head are aligned with these birefringent (fast and slow) axes when launching into the fiber, sensitivity to environmental effects is reduced and the input polarizations are maintained. For an ideal fiber and perfect launch conditions, the fiber input and output light could be described by the same wave equation. In reality, there is a small amount of polarization "leakage" between the fast and slow axes and small relative phase shifts introduced due to mechanical and environmental cable perturbations.

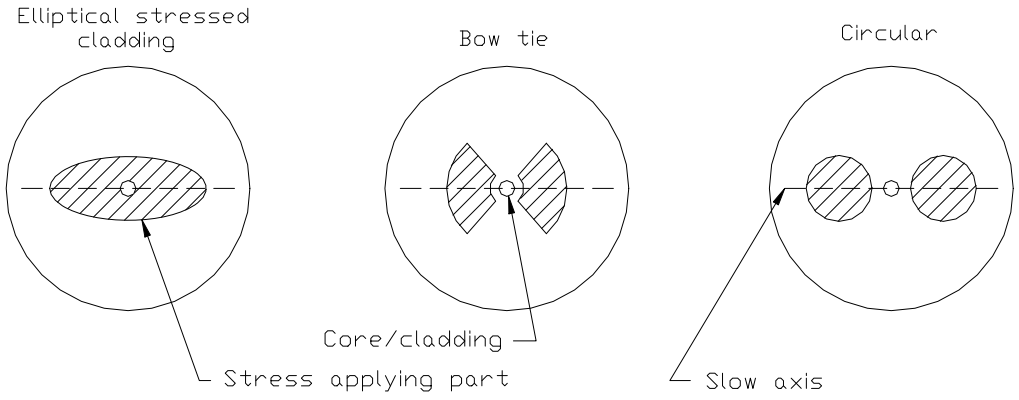

Figure 2.5.4: Single mode fibers.

Again referring to the heterodyne system shown in Figure 2.5.1, once the two orthogonal polarizations have traversed the Michelson interferometer (to introduce a relative phase shift between reference and measurement signals) and interfered at the Polaroid™, there is no longer any need to maintain the polarization state because the displacement information is now carried in the phase of the optical signal. Therefore, the light may now be carried on a high NA multimode (MM) fiber to the phase measuring electronics. Multimode fibers generally have a much larger core diameter and are easier to couple into than single mode fibers.

References

1. Musinski, D. "Interferometric Metrology: Linear and Angular Displacement", Tutorial at the 1997 Annual Meeting of the American Society for Precision Engineering, Norfolk, VA, October, 1997.
2. Sears, F., Zemansky, M., Young, H. College Physics, 7th Ed. Addison-Wesley Publishing, Co., New York, NY, 1991.
3. Pedrotti, F., Pedrotti, L. Introduction to Optics, 2nd Ed. Prentice Hall, Englewood Cliffs, NJ, 1993.
4. Feynman, R. QED The Strange Theory of Light and Matter, Princeton University Press, Princeton, NJ, 1985.
5. Selberg, L. "Interferometric Metrology: An Introduction", Tutorial at the 1994 Annual Meeting of the American Society for Precision Engineering, Cincinnati, OH, October, 1994.
6. Johnson, B. Optics and Optical Instruments, Dover Publications, Inc., New York, NY, 1960.
7. Slocum, A. Precision Machine Design, Prentice-Hall, Inc., Englewood Cliffs, NJ, 1992.
8. Thomson, W. Mechanical Vibrations, 2nd Ed., Prentice-Hall, Inc., Englewood Cliffs, NJ, 1958.
9. Beckwith, J. Personal conversations at Lawrence Livermore National Laboratory, Livermore, CA, May-August, 1997.
10. "Projects in Fiber Optics: Companion Applications Handbook", Newport Model #FKP, Newport Corporation, Irvine, CA, 1988.
11. Sezerman, O., Best, G. "Accurate alignment preserves polarization", *Laser Focus World*, Vol. 33, No. 12, December, 1997, pp. S27-S30.
12. Srivastava, R. "EEL 4445: Class Notes", University of Florida, Gainesville, FL, Spring, 1998.

